Regulate Higher-order Organization through the Synergy of Two Self-sorted Assembly

Wei Ji,[a] Shijin Zhang,[a] Sachie Yukawa,[a] Shogo Onomura,[b] Toshio Sasaki,[c] and Ye Zhang*[a]

Abstract: Extracellular matrix (ECM) is the natural fibrous scaffold that regulates cell behaviors in a hierarchical manner. By mimicking the dynamic and reciprocal interactions between ECM and cells, we developed higher-order molecular self-assembly (SA) mediated through the dynamic growth of scaffold like nanostructures assembled by different molecular components. Two self-sorted coumarin-based gelators, one peptide molecule and one benzoate molecule that self-assemble into nanofibers and nanobelts with different dynamic profiles, respectively, are designed and synthesized. Upon the dynamic growth of fibrous scaffold assembled from peptide gelators, benzoate gelators assembled nanobelts transform into layer-by-layer nanosheet reaching 9-fold increase in height. Using light and enzyme, we can modify the growth of scaffold spatial-temporally leading to *in situ* height regulation of the higher-order architecture. Exploration of this exceptional case opens the window for generalized method of advanced materials construction.

Molecular self-assembly (SA) has been emerged into chemical synthesis as an effective strategy for bottom-up fabrication of nanostructures.[1] Although the mimicry of living system for nano-fabrication has made many accomplishments, the insuperable barrier still remains between the synthetic self-assembly and biological design. One of the top challenges is to develop spontaneous higher-order organization across extended length scale. By coupling interactive components in a time- and scale-dependent manner, scientists developed mesoscale self-assembly (MESA)[2] as bottom-up fabrication of higher-order architecture with complex form and hierarchy.[3] Nowadays, MESA has become main path to hierarchical hybrid (inorganic-organic systems) architecture. Although hierarchical SA is fundamental in living organisms to transform molecules into high-order materials with advanced functions,[4] the bottom-up construction of single component hierarchical architecture is still challenging in synthetic SA.

Following the inspiration of the reciprocal interaction between cells and extracellular matrix (ECM)[5] in which cells continually remodel the ECM presented in their microenvironment and these dynamic modification of ECM direct the group behaviors of cells, we developed a bottom-up construction method of transformation of single component synthetic molecules into higher-order organization instructed by a dynamic growth of molecular self-assembled scaffold. As shown in Figure 1, we design two molecules, one self-assembles into brick like structure applicable for higher-order organization, and the other one self-assembles into fibrous scaffold. When they are mixed together, they self-assemble in self-sorted manner.[6] Similar to building construction, upon the growth of the scaffold, supported by the surface interactions between the nanostructures, bricks transform into higher-order architecture. A spatial-temporal modification of the scaffold growth leads to a height regulation of the final hierarchical architecture.

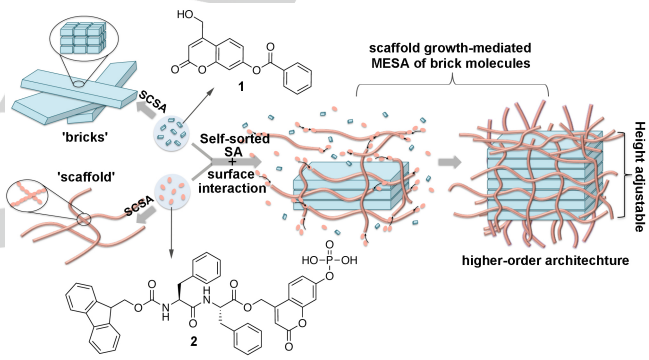

Figure 1. Schematic illustration of higher-order organization through the synergy of two self-sorted assembly with molecular structures of gelators **1** and **2**.

The exploration of a pair of molecules succeeding such hierarchical assembly has to consider several key aspects. First, different driving forces are expected for multi-stage assembly. At nanoscale level, orthogonal driving forces dominate assembly in a self-sorted manner forming nanostructures as basic building blocks. At mesocale level, the surface forces between these nanostructures determine how they become assembled for higher-order organization.[2d] Therefore, molecules that have certain similar structural components leading to potential surface interaction, also balanced with distinct structural components leading to orthogonal driving force for self-sorted SA are ideal. Second, optimal morphology combination obtained from self-sorted SA is required. Third, the stimuli-responsive SA of scaffold will provide the possibilities for further regulation of higher-order construction. Accordingly, we built up a small library of coumarin-derived gelators[7] with light responses,[8] and found a proper pair of coumarin derivatives, **1** and **2** (Figure 1), for higher-order organization.

Both gelators self-assemble forming self-supported hydrogels beyond critical concentrations (Figure S1)**.** Immediate phase transition happened to **1** resulting into an opaque gel. A relatively slower phase transition of **2** was observed leading to a transparent gel after 48 s. The morphologies of single component self-assembly (SCSA) were examined using

[a] Dr. Wei Ji, Mr. Shijin Zhang, Ms. Sachie Yukawa, Prof. Dr. Ye Zhang
Bioinspired Soft Matter Unit
Okinawa Institute of Science and Technology Graduate University
1919-1 Tancha, Onna-son, Okinawa, 904-0495, Japan
E-mail: ye.zhang@oist.jp
[b] Mr. Shogo Onomura
Shimadzu Techno-Research Co. Ltd., 1 Nishinokyo, Nakagyo-ku, Kyoto, 604-8436, Japan
[c] Mr. Toshio Sasaki
Imaging Section
Okinawa Institute of Science and Technology Graduate School
Supporting information for this article is given via a link at the end of the document.

scanning electron microscopy (SEM) and transmission electron microscopy (TEM). **1** self-assembled into rigid nanobelts with wide range of width from 150 to 250 nm (Figure 2A and 2B), good for basic building block construction for higher-order organization. While **2** self-assembled into well-defined flexible nanofibers with width of 7-8 nm (Figure 2C and 2D), good for scaffold construction. Apparently, the distinct morphologies of two SCSA nanostructures make them distinguishable from each other under microscopes.

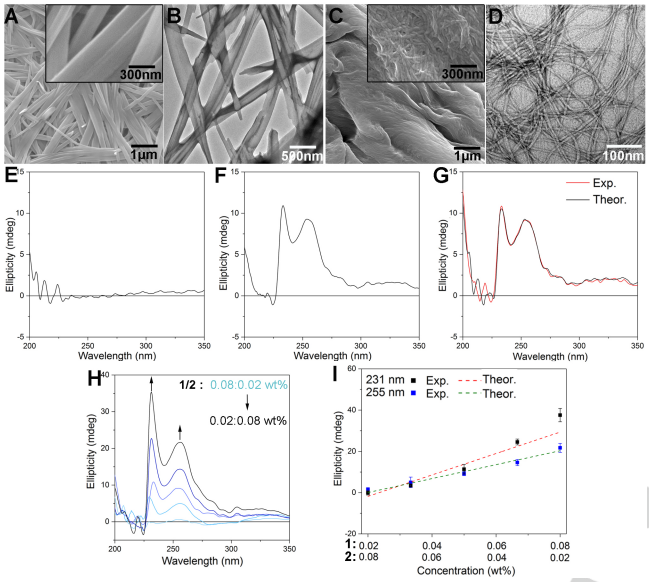

Figure 2. SEM (A) and TEM (B) images of SA of **1** in H_2O/DMSO (v/v = 9:1) at concentration of 0.8 wt%. SEM (C) and TEM (D) images of SA of **2** in H_2O/DMSO (v/v = 9:1) at concentration of 0.8 wt%. CD spectra of **1** (0.05 wt%) (E), **2** (0.05 wt%) (F) and **1**/**2** mixture ([**1**] = 0.05 wt%, [**2**] = 0.05 wt%) (G) in H_2O/DMSO (v/v = 9:1). Exp. and Theor. represent experimental and theoretical CD spectra, respectively. (H) CD spectra of **1**/**2** mixture at various ratios in H_2O/DMSO (v/v = 9:1). (I) Plots of CD intensities of **1**/**2** mixture at 231nm, and 255 nm versus mixing ratios from H. Theoretical lines were calculated from the CD intensities of each component at various concentrations. Data represent mean ± standard deviation of the mean (n = 3).

Self-sorted nanostructures would be expected from the mixture of **1** and **2** because of their potentially orthogonal driving forces for SA including π-π interaction between coumarins and C-H···O hydrogen bonding for **1** confirmed by the single crystal packing modes (Figure S2),[7b] and different π-π interaction and N-H···O hydrogen bonding for dipeptide-based gelator **2**.[9] The orthogonality of **1** and **2** was evaluated using CD spectroscopy studying the SA induced Cotton effect.[6e] Being distinguishable from the CD spectrum of **1** (Figure 2E), the CD spectrum of **2** shows two positive peaks (Figure 2F). The one at 231 nm arises from the peptides subunit. And the 255 nm peak arises from the exciton coupling induced by J-aggregation of the fluorenyl group and coumarin subunit (Figure S3).[9c, 9f, 9g] The CD spectrum from a 1:1 mixture of **1** and **2** (experimental) is almost identical to the simple sum (theoretical) of two single-component spectra (Figure 2G). It suggests that **1** and **2** form self-sorted nanostructures. We also varied the mixing ratio of **1**/**2** from 4:1 to 1:4, and monitored the CD spectra. As shown in Figure 2H, the peaks at 231 nm and 255 nm rise linearly by increasing the proportion of **2**. The experimental results agree with theoretical lines calculated from the changes in single-component CD spectra (Figure 2I, and Figure S4). The CD spectra indicate that the nanostructures are assembled from single component, scarcely interfere with one another at various mixing ratios. The FTIR spectrum from a 1:1 mixture of **1** and **2** (experimental) is almost identical to the simple sum (theoretical) of two single-component spectra (Figure S5), which also suggests self-sorted SA.

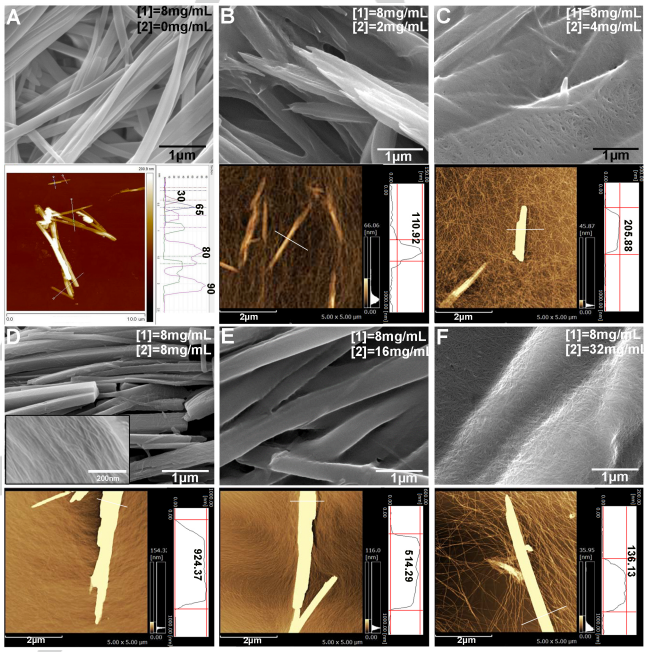

Figure 3. SEM images and the correlated AFM images with height profiles of SCSA of **1** (A) and mixture of **1** (8mg/mL) with **2** at various concentrations, from 2mg/mL (B), 4 mg/mL (C), 8 mg/mL (D), 16 mg/mL (E), to 32 mg/mL (F) in H_2O/DMSO (v/v = 9:1), respectively. The inset SEM image in Figure D represents the section structure of layer-by-layer nanosheet.

To evaluate the influence of scaffold growth on higher-order organization of **1**, we examined the morphology change of **1**/**2** mixture at various ratios by SEM and atomic force microscopy (AFM) (Figure 3). We changed the proportion of **2**, while the concentration of **1** was maintained at 8 mg/mL. SEM images show prominent objects surrounded by nanofibers with identical morphology to the SCSA of **2**. Comparing to the thin nanobelts with height from 30 to 90 nm formed by SCSA of **1** (Figure 3A), the SA of **2** facilitates the SA of **1** forming higher objects. And depending on the proportion of **2**, SA of **1** forms similar objects with clearly different height at various heterogeneities (Figure S6). For example, when [**2**] = 2 mg/mL (**1**/**2** = 4/1 w/w), nanobelts achieved height of 110 nm (Figure 3B). When [**2**] increased to 4 mg/mL (**1**/**2** = 2/1 w/w), the height of nanobelt reached 205 nm (Figure 3C). Once [**2**] equaled to 8 mg/mL (**1**/**2** = 1/1 w/w), the height of nanobetls increased more reaching more than 920 nm (Figure 3D). The section SEM demonstrated a layer-by-layer architecture suggesting a MESA path to the higher-order organization (Figure S7). Over-increasing the

concentration of **2** down regualted the height of prominent objects. At [**2**] = 16 mg (**1**/**2** = 1/2 w/w), SA of **1** formed nanobelts with 514 nm height (Figure 3E). Once [**2**] increased to 32 mg/mL (**1**/**2** = 1/4 w/w), the height of the nanobelts reduced to 136 nm (Figure 3F). And an increase in heterogeneity always complied with the formation of higher height objects.

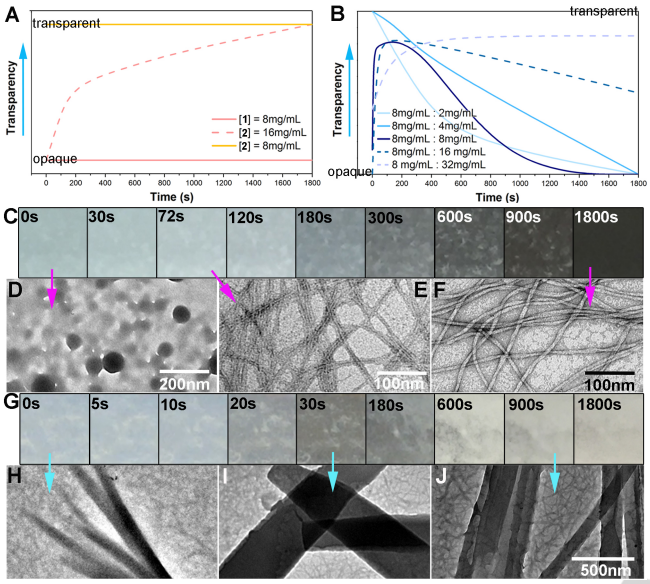

Figure 4. Estimated time-dependent transparency profiles of SCSA (A), and SA of **1**/**2** mixture. Time lapse optical images of **2** in H_2O/DMSO (v/v = 9:1) at concentration of 16 mg/mL (C), and the correlated TEM images at 0 s (D), 72 s (E) and 1800 s (F). Time lapse optical images of **1**/**2** mixture in H_2O/DMSO (v/v = 9:1) at concentration of 8 mg/mL of each (G), and the correlated TEM images at 0 s (H), 30 s (I) and 1800 s (J).

To study the SA kinetic profiles of both single component and mixture,[10] we summarized the phase transitions based on optical and TEM images (Figure 4 and S8). At 8 mg/mL, **1** self-assembled into opaque gel with nanobelt structure immediately, while **2** formed into transparent gel at the same concentration with fibrous nanostructures instantly. By raising the concentration to 16 mg/mL, phase transition induced by SCSA of **2** was visualized, from opaque emulsion to transparent gel in a 30 min time frame. Time-lapse TEM images indicate that the SA of **2** transformes from irregular aggregates, through 4 nm width nanofibers, eventually stabilized as 7-8 nm width nanofibers (Figure 4D-F). Apparently, increasing the concentration of **2** can extend the time frame for stabilized fibrous structure. When 2 mg/mL of **2** was mixed with 8 mg/mL of **1**, a transformation from clear solution to opaque gel was observed. By increasing the concentration of **2** to 4 mg/mL, the opacity transition was slightly postponed. At [**2**] = 8 mg/mL, the mixture went through a full transition cycle of opaque-transparent-opaque, leading into the highest layer-by-layer nanostructure among the five mixtures (Figure 4G). Time-lapse TEM images suggest a morphology transition from the combination of irregular nanofibers/nanobelts through uniformed nanofibers/nanobelts into uniformed nanofibers/layered nanobelts (Figure 4H-J). Besides the regulation of higher order organization of **1** by SA of **2**, the existence of **1** also affects the phase transition of **2** suggesting a reciprocal interaction between **1** and **2**. Increasing the concentration of **2** to 16 mg/mL or 32 mg/mL in **1**/**2** mixture ([**1**] = 8 mg/mL) caused incompletion of transition cycle. The mixture ended into translucent gels with unevenly distributed white aggregates. And nanostructures with reduced height were obtained. The experimental results suggest that the coexistence of **1** and **2** affects each other's SA reciprocally. The density and morphology of the scaffold formed through SA of **2** at both static state and kinetic transition process regulate the height of the higher-order architecture of **1** in a collective fashion.

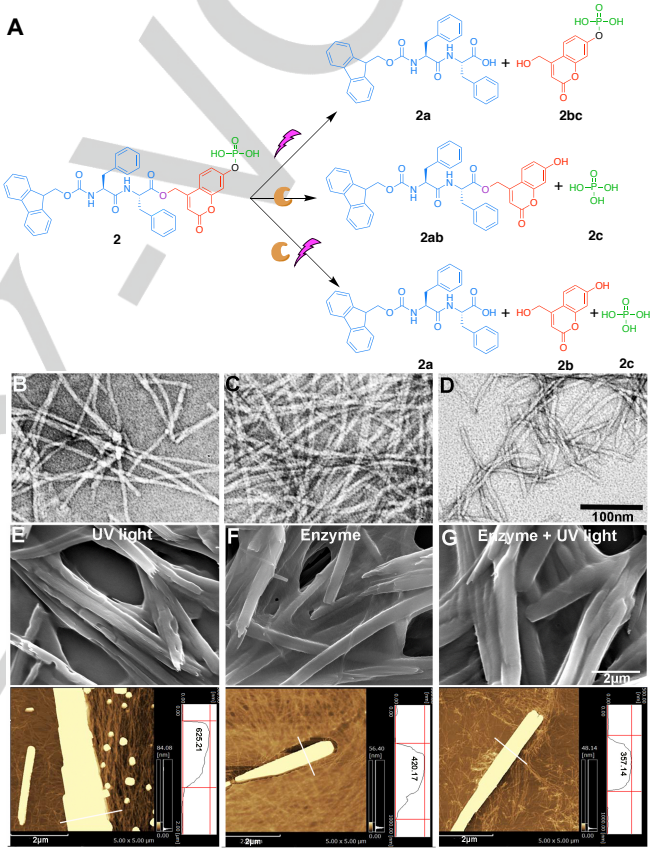

Figure 5. (A) UV light and/or enzyme triggered degradations of **2**. The TEM images of **2** (100 μM) in H_2O/DMSO (v/v = 9:1) under UV light (B), enzyme treatment (C), both UV light/enzyme treatment (D) for 30 min. SEM images and correlated AFM images with height profiles of **1**/**2** mixture in H_2O/DMSO (v/v = 9:1) at concentration of 8 mg/mL of each under UV light (E), enzyme treatment (F), and UV light/enzyme treatment (G), respectively.

UV light and enzyme can be applied as external stimuli to convert **2** into various combinations of chemical structures (Figure 5A and S9) leading into scaffold modification at molecular level. For example, **2** is cleaved into **2a** and **2bc** under UV light resulting into short fibrils (Figure 5B) with similar width to the nanofibers formed in SCSA of **2** (Figure 2D). Treated by enzyme (alkaline phosphatase),[11] **2** converted into **2ab** and **2c** assembled into similar nanofibers (Figure 5C) as the SCSA of **2**. Under both stimuli, **2** degraded into **2a**, **2b**, and **2c**

leading to even shorter nanofibers (Figure 5D). Regarding the difference among their molecular structures, **2a**, **2bc**, **2ab**, and **2b** definitely have different driving forces for SA. The difference in molecular packing of the SA also leads to different surface interactions affecting higher-order organization of **1**. We introduced *in situ* scaffold modification to the MESA of **1** (8mg/mL)/**2** (8mg/mL) mixture by applying the stimuli before SA. Compare to unmodified mixture with the same components, *in situ* external stimuli-induced scaffold modification affected the SA of **1** leading to nanobelts with different height and heterogeneity (Figure S10). For example, under the UV-light irradiation, the height of nanobelts formed by SA of **1** reduced to 625 nm (Figure 5E). Treated by enzyme, the height of nanobetls reduced to 420 nm (Figure 5F). Under both stimuli, SA of **1** formed nanobelts with only 354nm height (Figure 5G). Since both UV light irradiation and enzyme addition show no impacts on the SCSA of **1** (Figure S11), these results indicate that the *in situ* structure modification of scaffold (SA of **2**) also regulates the higher-order organization of **1**.

ECM is dynamic and complex. Each tissue has dedicated ECM with specific mechanical and biological properties that regulate cell behaviour. Scientists developed materials fabrication to mimic the morphology and activity of ECM in a static manner for tissue engineering. Unfortunately, the most fascinating feature −the dynamic property of ECM involved in its advanced functionality is still missing. Adopting the concept of nanoarchitetonics,[12] by selecting a proper pair of self-sorted synthetic molecules, we discovered that the dynamic molecular SA into fibrous nanostructures could perform as a living scaffold facilitating the hierarchical assembly of the other molecule into higher-order architecture. It's a feasible biomimetic design for single-component hierarchical SA. Exploration of the exceptional case for higher-order organization will open the window for generalized method of advanced materials construction beneficial to biomimetic design.

Acknowledgements

The research is supported by Okinawa Institute of Science and Technology Graduate University and Takeda Science Foundation. The AFM images were captured in Shimadzu Techno-Research Co. Ltd.

Keywords: self-assembly • self-sorting • gelator • coumarin• higher-order organization

[1] a) G. M. Whitesides, M. Boncheva, *Proc. Natl. Acad. Sci. USA* **2002**, 99, 4769; b) G. M. Whitesides, J. P. Mathias, C. T. Seto, *Science* **1991,** *254*, 1312; c) E. Gazit, *Chem. Soc. Rev.* **2007**, *36*, 1263; d) X. H. Yan, P. L. Zhu, J. B. Li, *Chem. Soc. Rev.* **2010**, *39*, 1877. e) J. Y. Cheng, A. M. Mayes, C. A. Ross, *Nat. Mater.* **2004**, 3, 823.

[2] a) N. Bowden, I. S. Choi, B. A. Grzybowski, G. M. Whitesides, *J. Am. Chem. Soc.* **1999**, *121*, 5373; b) N. Bowden, S. R. J. Oliver, G. M. Whitesides, *J. Phys. Chem. B* **2000**, *104*, 2714; c) N. B. Bowden, M. Weck, I. S. Choi, G. M. Whitesides, *Accounts Chem. Res.* **2001**, *34*, 231; d) H. Colfen, S. Mann, *Angew. Chem., Int. Ed.* **2003**, *42*, 2350; *Angew. Chem.* **2003**, *115*, 2452; e) M. Li, B. Lebeau, S. Mann, *Adv. Mater.* **2003**, *15*, 2032; f) S. A. Semerdzhiev, D. R. Dekker, V. Subramaniam, M. M. Claessens, *ACS Nano* **2014**, *8*, 5543.

[3] a) A. H. Groschel, A. H. E. Muller, *Nanoscale* **2015**, *7*, 11841; b) S. Whitelam, *Physics* **2014**, *7*, 62.

[4] R. P. Sear, I. Pagonabarraga, A. Flaus, *Bmc Biophys* **2015**, *8*, 4.

[5] a) F. Gattazzo, A. Urciuolo, P. Bonaldo, *Bba-Gen Subjects* **2014**, *1840*, 2506; b) C. Frantz, K. M. Stewart, V. M. Weaver, *J. Cell Sci.* **2010**, *123*, 4195; c) S. H. Kim, J. Turnbull, S. Guimond, *J. Endocrinol* **2011**, *209*, 139.

[6] a) K. Pandurangan, J. A. Kitchen, S. Blasco, E. M. Boyle, B. Fitzpatrick, M. Feeney, P. E. Kruger, T. Gunnlaugsson, *Angew. Chem., Int. Ed.* **2015,** *54*, 4566; *Angew. Chem.* **2015**, *127*, 4649; b) K. L. Morris, L. Chen, J. Raeburn, O. R. Sellick, P. Cotanda, A. Paul, P. C. Griffiths, S. M. King, R. K. O'Reilly, L. C. Serpell, D. J. Adams, *Nat. Commun.* **2013**, *4*, 1480; c) E. R. Draper, B. Dietrich, D. J. Adams, *Chem. Commun.* **2017,** *53*, 1868; d) E. R. Draper, D. J. Adams, *Nat. Chem.* **2016**, *8*, 737. e) S. Onogi, H. Shigemitsu, T. Yoshii, T. Tanida, M. Ikeda, R. Kubota, I. Hamachi, *Nat. Chem.* **2016**, *8*, 743; f) M. M. Smith, D. K. Smith, *Soft Matter* **2011**, *7*, 4856; g) D. J. Cornwell, O. J. Daubney, D. K. Smith, *J. Am. Chem. Soc.* **2015**, *137*, 15486; h) F. Wang, C. Y. Han, C. L. He, Q. L. Zhou, J. Q. Zhang, C. Wang, N. Ling, F. H. Huang, *J. Am. Chem. Soc.* **2008**, *130*,11254; i) M. M. Safont-Sempere, G. Fernandez, F. Wurthner, *Chem. Rev.* **2011**, *111*, 5784; j) W. Jiang, C. A. Schalley, *Proc. Natl. Acad. Sci. U.S.A.* **2009,** *106*, 10425; k) Z. F. He, W. Jiang, C. A. Schalley, *Chem. Soc. Rev.* **2015,** *44*, 779; l) L. L. Yan, C. H. Tan, G. L. Zhang, L. P. Zhou, J. C. Bunzli, Q. F. Sun, *J. Am. Chem. Soc.* **2015**, *137*, 8550.

[7] a) W. Ji, G. F. Liu, Z. J. Li, C. L. Feng, *ACS Appl. Mater. Inter.* **2016**, *8*, 5188; b) W. Ji, S. J. Zhang, G. A. Filonenko, G. Y. Li, T. Sasaki, C. L. Feng, Y. Zhang, *Chem. Commun.* **2017**, *53*, 4702; c) W. Ji, L. L. Li, O. Eniola-Adefeso, Y. M. Wang, C. T. Liu, C. L. Feng, *J. Mater. Chem. B* **2017**, *5*, 7790.

[8] a) D. Geissler, Y. N. Antonenko, R. Schmidt, S. Keller, O. O. Krylova, B. Wiesner, J. Bendig, P. Pohl, V. Hagen, *Angew. Chem., Int. Ed.* **2005**, *44*, 1195; *Angew. Chem.* **2005**, *117*, 1219; b) R. Schmidt, D. Geissler, V. Hagen, J. Bendig, *J. Phys. Chem. A* **2007**, *111*, 5768; c) Q. N. Lin, C. Y. Bao, S. Y. Cheng, Y. L. Yang, W. Ji, L. Y. Zhu, *J. Am. Chem. Soc.* **2012**, *134*, 5052; d) Q. N. Lin, Q. Huang, C. Y. Li, C. Y. Bao, Z. Z. Liu, F. Y. Li, L. Y. Zhu, *J. Am. Chem. Soc.* **2010**, *132*, 10645; e) T. Yoshii, M. Ikeda, I. Hamachi, *Angew. Chem, Int. Ed.* **2014**, *53*, 7264; *Angew. Chem.* **2014**, *126*, 7392; f) W. Ji, G. F. Liu, F. Wang, Z. Zhu, C. L. Feng, *Chem. Commun.* **2016**, *52*, 12574.

[9] a) A. M. Smith, R. J. Williams, C. Tang, P. Coppo, R. F. Collins, M. L. Turner, A. Saiani, R. V. Ulijn, *Adv Mater* **2008**, *20*, 37; b) J. Raeburn, T. O. McDonald, D. J. Adams, *Chem. Commun.* **2012**, *48*, 9355; c) K. Tao, A. Levin, L. Adler-Abramovich, E. Gazit, *Chem. Soc. Rev.* **2016**, *45*, 3935; d) C. Tang, A. M. Smith, R. F. Collins, R. V. Ulijn, A. Saiani, *Langmuir* **2009**, *25*, 9447; e) M. Fu, Q. Li, B. Sun, Y. Yang, L. Dai, T. Nylander, J. Li, *ACS Nano* **2017**, *11*, 7349; f) M. Kasha, H. R. Rawls, M. Ashraf El-Bayoumi, *Pure Appl. Chem.* **1965**, *11*, 371; g) A. Eisfeld, J. S. Briggs, *Chemical Physics*, **2006**, *324*, 376.

[10] P. Bairi, K. Minami, J. P. Hill, W. Nakanishi, L. K. Shrestha, C. Liu, K. Harano, E. Nakamura, K. Ariga, *ACS Nano*. **2016**, *10*, 8796.

[11] a) H. M. Wang, Z. Q. Q. Feng, A. Lu, Y. J. Jiang, H. Wu, B. Xu, *Angew. Chem., Int. Ed.* **2017**, *56*, 7579; *Angew. Chem.* **2017**, *129*, 7687; b) J. Zhou, X. Du, C. Berciu, H. He, J. Shi, D. Nicastro, B. Xu, *Chem* **2016**, *1*, 246; c) J. Zhou, X. W. Du, N. Yamagata, B. Xu, *J. Am. Chem. Soc.* **2016**, *138*, 3813; d) G. Li, T. Sasaki, S. Asahina, M. C. Roy, T. Mochizuki, K. Koizumi, Y. Zhang, *Chem* **2017,** *2*, 283.

[12] a) M. Aono, K. Ariga, *Adv. Mater.* **2016**, *28*, 989; b) M. Komiyama, K. Yoshimoto, M. Sisido, K. Ariga, *Bull. Chem. Soc. Jpn.* **2017**, *90*, 967.

Entry for the Table of Contents (Please choose one layout)

Layout 1:

COMMUNICATION

By mimicking the dynamic and reciprocal interactions between ECM and cells, we developed matrix growth-mediated self-assembly (SA) of organic molecules into higher-order organization. The dynamic self-assembly of nanofibrous scaffold facilitates the hierarchical assembly of rigid molecule into layered structure reaching 9-fold increase in height.

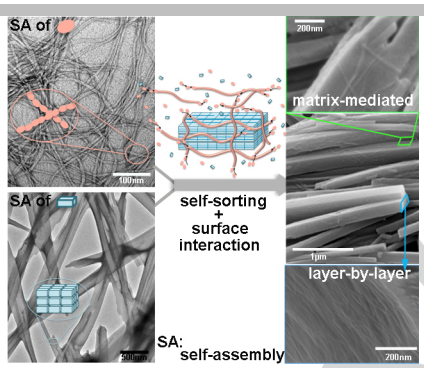

*Wei Ji, Shijin Zhang, Sachie Yukawa, Shogo Onomura, Toshio Sasaki, and Ye Zhang**

Page No. – Page No.

Regulate Higher-order Organization through the Synergy of Two Self-sorted Assembly